

Computational Design of Chemical Nanosensors: Metal Doped Carbon Nanotubes

J. M. García-Lastra^{1,2} ^{*} D. J. Mowbray^{1,2}, K. S. Thygesen², A. Rubio^{1,3}, and K. W. Jacobsen²

¹*Nano-Bio Spectroscopy group and ETSF Scientific Development Centre,*

Dpto. Física de Materiales, Universidad del País Vasco,

Centro de Física de Materiales CSIC-UPV/EHU- MPC and DIPC, Av. Tolosa 72, E-20018 San Sebastián, Spain

²*Center for Atomic-scale Materials Design, Department of Physics,*

Technical University of Denmark, DK-2800 Kgs. Lyngby, Denmark

³*Fritz-Haber-Institut der Max-Planck-Gesellschaft, Berlin, Germany*

We use computational screening to systematically investigate the use of transition metal doped carbon nanotubes for chemical gas sensing. For a set of relevant target molecules (CO, NH₃, H₂S) and the main components of air (N₂, O₂, H₂O), we calculate the binding energy and change in conductance upon adsorption on a metal atom occupying a vacancy of a (6,6) carbon nanotube. Based on these descriptors, we identify the most promising dopant candidates for detection of a given target molecule. From the fractional coverage of the metal sites in thermal equilibrium with air, we estimate the change in the nanotube resistance per doping site as a function of the target molecule concentration assuming charge transport in the diffusive regime. Our analysis points to Ni-doped nanotubes as candidates for CO sensors working under typical atmospheric conditions.

PACS numbers: 73.63.-b, 68.43.-h, 73.50.Lw

The ability to detect small concentrations of specific chemical species is fundamental for a variety of industrial and scientific processes as well as for medical applications and environmental monitoring [1]. In general, nanostructured materials should be well suited for sensor applications because of their large surface to volume ratio which makes them sensitive to molecular adsorption. Specifically, carbon nanotubes (CNT) [2] have been shown to work remarkably well as detectors of small gas molecules. This has been demonstrated both for individual CNTs [3–8] as well as for CNT networks [9, 10].

Pristine CNTs are known to be chemically inert – a property closely related to their high stability. As a consequence, only radicals bind strong enough to the CNT to notably affect its electrical properties [2, 5, 11–13]. To make CNTs attractive for sensor applications thus requires some kind of functionalization, e.g. through doping or decoration of the CNT sidewall [13–21]. Ideally, this type of functionalization could be used to control not only the reactivity of the CNT but also the selectivity towards specific chemical species.

In this work we consider the possibility of using CNTs doped by 3d transition metal atoms for chemical gas sensing. We use computational screening to systematically identify the most promising dopant candidates for detection of three different target molecules (CO, NH₃, H₂S) under typical atmospheric conditions. The screening procedure is based on the calculation of two microscopic descriptors: the binding energy and scattering resistance of the molecules when adsorbed on a doped CNT. These two quantities give a good indication of the gas coverage and impact on the resistance. For the most promising candidates we then employ a simple thermodynamic model of the CNT sensor. In this model, the binding energies are used to obtain the fractional coverage of the metallic sites as a function of the target molecule concentration under ambient conditions. Under the assumption of transport in the diffusive rather than localization regime, the

change in CNT resistivity may then be obtained from the calculated coverages and single impurity conductances.

We find that oxidation of the active metal site passivates the sensor in the case of doping by Ti, V, Cr, and Mn under standard conditions (room temperature and 1 bar of pressure). Among the remaining metals, we identify Ni as is the most promising candidate for CO detection. For this system the change in resistance per active site is generally significant ($>1\ \Omega$) for small changes in CO concentration in the relevant range of around 0.1–10 ppm. Our approach is quite general and is directly applicable to other nanostructures than CNTs, other functionalizations than metal doping, and other backgrounds than atmospheric air.

All total energy calculations and structure optimizations have been performed with the real-space density functional theory (DFT) code GPAW [22] which is based on the projector augmented wave method. We use a grid spacing of 0.2 Å for representing the density and wave functions and the PBE exchange correlation functional [23]. Transport calculations for the optimized structures have been performed using the non-equilibrium Green's function method [24] with an electronic Hamiltonian obtained from the SIESTA code [25] in a double zeta polarized (DZP) basis set. Spin polarization has been taken into account in all calculations.

Metallic doping of a (6,6) CNT has been modeled in a supercell containing six repeated minimal unit cells along the CNT axis (dimensions: 15 Å \times 15 Å \times 14.622 Å). For this size of supercell a Γ -point sampling of the Brillouin zone was found to be sufficient. The formation energy for creating a vacancy (VC) occupied by a transition metal atom (M) was calculated using the relation

$$E_{\text{form}}[\text{M@VC}] = E[\text{M@VC}] + nE[\text{C}] - E[\text{M@NT}] \quad (1)$$

where $E[\text{M@VC}]$ is the total energy of a transition metal atom occupying a vacancy in the nanotube, n is the number of carbon atoms removed to form the vacancy, $E[\text{C}]$ is the energy per carbon atom in a pristine nanotube, and $E[\text{M@NT}]$

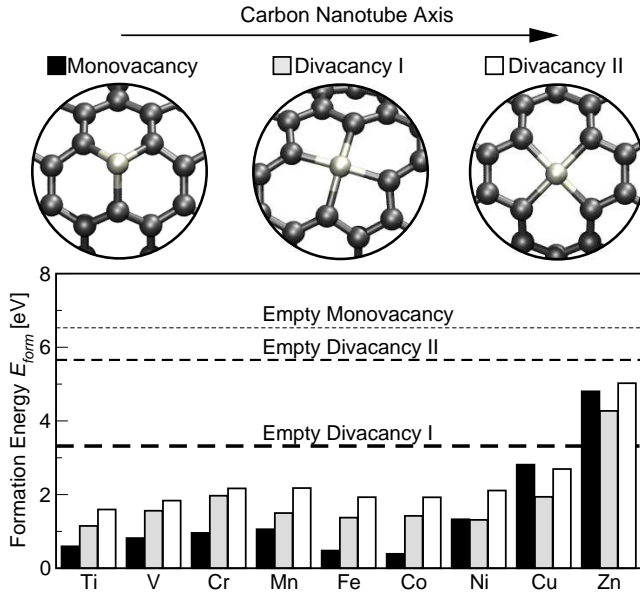


FIG. 1: Structural schematics and formation energy for a 3d transition metal occupied monovacancy (black), divacancy I (gray), or divacancy II (white) in a (6,6) carbon nanotube. Formation energies of the empty vacancies are indicated by dashed lines.

is the total energy of the pristine nanotube with a physisorbed transition metal atom. We have considered the monovacancy and two divacancies shown in Fig. 1. The energy required to form an empty vacancy is obtained from

$$E_{\text{form}}[\text{VC}] = E[\text{VC}] + nE[\text{C}] - E[\text{NT}], \quad (2)$$

where $E[\text{VC}]$ is the total energy of the nanotube with a vacancy of n atoms.

The calculated formation energies for the 3d transition metals are shown in Fig. 1. From the horizontal lines we see that both divacancies are more stable than the monovacancy. This may be attributed to the presence of a two-fold coordinated C atom in the monovacancy, while all C atoms remain three-fold coordinated in the divacancies. When a transition metal atom occupies a vacancy, the strongest bonding to the C atoms is through its d orbitals [26]. For this reason, Cu and Zn, which both have filled d -bands, are rather unstable in the CNT. For the remaining metals, adsorption in the monovacancies leads to quite stable structures. This is because the three-fold coordination of the C atoms and the CNT's hexagonal structure are recovered when the metal atom is inserted. On the other hand, metal adsorption in divacancies is slightly less stable because of the resulting pentagon defects, see upper panel in Fig. 1. A similar behaviour has been reported by Krasheninnikov *et al.* for transition metal atoms in graphene [21].

The adsorption energies for N_2 , O_2 , H_2O , CO , NH_3 , and H_2S on the metallic site of the doped (6,6) CNTs are shown in Fig. 2(a). The adsorption energy of a molecule X is defined by

$$E_{\text{ads}}[X@\text{M@VC}] = E[X@\text{M@VC}] - E[X] - E[\text{M@VC}], \quad (3)$$

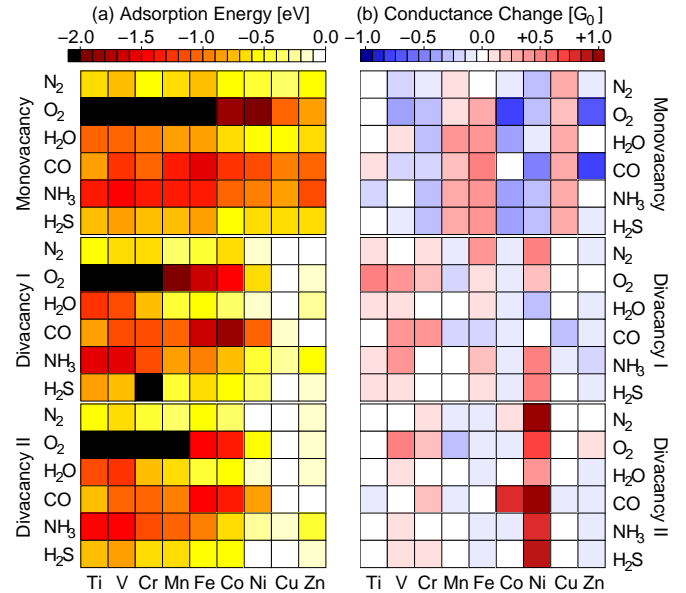


FIG. 2: Calculated (a) adsorption energy E_{ads} in eV and (b) change in conductance ΔG in units of $G_0 = 2e^2/h$ for N_2 , O_2 , H_2O , CO , NH_3 , and H_2S on 3d transition metals occupying a monovacancy (top), divacancy I (middle), and divacancy II (bottom) in a (6,6) carbon nanotube.

where $E[X@\text{M@VC}]$ is the total energy of molecule X on a transition metal atom occupying a vacancy, and $E[X]$ is the gas phase energy of the molecule.

From the adsorption energies plotted in Fig. 2(a), we see that the earlier transition metals tend to bind the adsorbates stronger than the late transition metals. The latest metals in the series (Cu and Zn) bind adsorbates rather weakly in the divacancy structures. We also note that O_2 binds significantly stronger than any of the three target molecules on Ti, V, Cr, and Mn (except for Cr in divacancy I where H_2S is found to dissociate). Active sites containing these metals are therefore expected to be completely passivated if oxygen is present in the background. Further, we find H_2O is rather weakly bound to most of the active sites. This ensures that these types of sensors are robust against changes in humidity.

In thermodynamic equilibrium [27], the coverage of the active sites follows from

$$\Theta[X] = \frac{K[X]C[X]}{1 + \sum_Y K[Y]C[Y]}, \quad (4)$$

where $K = k_+/k_-$ is the ratio of forward and backward rate constants for the adsorption reaction,

$$K[X] = \exp \left[-\frac{E_{\text{ads}}[X] + TS[X]}{k_B T} \right]. \quad (5)$$

In these expressions $C[X]$ is the concentration of species X , $S[X]$ is its gas phase entropy and T is the temperature. Experimental values for the gas phase entropies have been taken from Ref. [28].

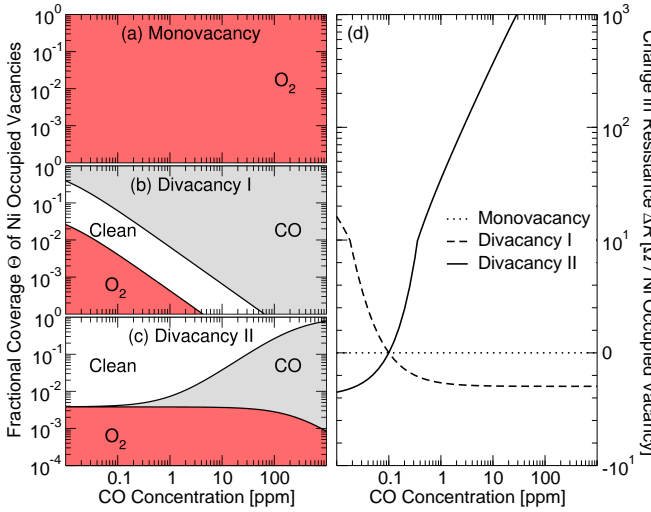


FIG. 3: Fractional coverage Θ in thermal equilibrium of Ni in a (a) monovacancy, (b) divacancy I, (c) divacancy II and (d) change in resistance ΔR per dopant site as a function of CO concentration in a background of air at room temperature and 1 bar of pressure. The reference concentration of CO is taken to be $C_0 = 0.1$ ppm. Note the change from linear to log scale on the y -axis at $\Delta R = 10 \Omega$.

For a given background composition we may thus estimate the fractional coverages for each available adsorbate for a given type of doping. As an example, Fig. 3(a)-(c) shows the fractional coverage of a Ni atom occupying a monovacancy, divacancy I, and divacancy II, versus CO concentration in a background of air at room temperature and 1 bar of pressure. Due to the relatively small binding energy of N_2 and H_2O as compared to O_2 and CO, all Ni sites will be either empty or occupied by O_2 or CO. In particular, Ni in a monovacancy (top panel of Fig. 3) will be completely oxidized for all relevant CO concentrations. For the Ni occupied divacancy II structures we find the coverage of CO changes significantly around toxic concentrations (~ 10 ppm).

To estimate the effect of adsorbates on the electrical conductance of doped CNTs, we first consider the change in conductance when a single molecule is adsorbed on a metal site of an otherwise pristine CNT. In Fig. 2(b) we show the calculated change in conductance relative to the metal site with no adsorbate. In contrast to the binding energies, there are no clear trends in the conductances. The sensitivity of the conductance is perhaps most clearly demonstrated by the absence of correlation between different types of vacancies, i.e. between the three panels in Fig. 2(b). Close to the Fermi level, the conductance of a perfect armchair CNT equals $2G_0$. The presence of the metal dopant leads to several dips in the transmission function known as Fano antiresonances [20]. The position and shape of these dips depend on the d -levels of the transition metal atom, the character of its bonding to the CNT, and is further affected by the presence of the adsorbate molecule. The coupling of all these factors is very complex and makes it difficult to estimate or rationalize the value of the conductance. For the spin polarized cases, we use the spin-averaged

conductances, i.e. $G = (G_\uparrow + G_\downarrow)/2$.

Next, we estimate the resistance of a CNT containing several impurities (a specific metal dopant with different molecular adsorbates). Under the assumption that the electron phase-coherence length, l_ϕ , is smaller than the average distance between the dopants, d , we may neglect quantum interference and obtain the total resistance by adding the scattering resistances due to each impurity separately. The scattering resistance due to a single impurity is given by

$$R_s(X) = 1/G(X) - 1/(2G_0), \quad (6)$$

where $G(X)$ is the Landauer conductance of the pristine CNT with a single metal dopant occupied by molecule X and $1/(2G_0)$ is the contact resistance of a (6,6) CNT.

We may now obtain the total resistance per dopant site relative to the reference background signal as a function of the target molecule concentration

$$\frac{\Delta R}{N} \approx \sum_X R_s(X)(\Theta[X, C] - \Theta[X, C_0]), \quad (7)$$

where N is the number of dopants, $\Theta[X, C]$ is the fractional coverage of species X at concentration C of the target and C_0 is the reference concentration. Notice that the contact resistance drops out as we evaluate a change in resistance.

In Fig. 3(d) we show the change in resistance calculated from Eq. (7) as a function of CO concentration for Ni occupying the three types of vacancies. The background reference concentration of CO is taken to be $C_0 = 0.1$ ppm. For the monovacancy there is very little change in resistivity. This is because most active sites are blocked by O_2 at relevant CO concentrations, as shown in the upper panel of Fig. 3. For Ni in the divacancies there is, however, a change in resistance on the order of 1Ω per site. For concentrations above ~ 1 ppm, the CO coverage of Ni in the divacancy II increases dramatically and this leads to a significant increase in resistance.

We now return to the discussion of the validity of Eq. (7). As mentioned, the series coupling of individual scatterers should be valid when $l_\phi < d$. However, even for $l_\phi > d$ and assuming that the Anderson localization length, l_{loc} in the system exceeds l_ϕ , Eq. (7) remains valid if one replaces the actual resistance R by the sample averaged resistance $\langle R \rangle$ [29]. At room temperature under ambient conditions, interactions with external degrees of freedom such as internal CNT phonons and vibrational modes of the adsorbed molecules would rapidly randomize the phase of the electrons. Therefore Eq. (7) should certainly be valid in the limit of low doping concentrations. On the other hand, the total number of dopants, N , should be large enough for the statistical treatment of the coverage to hold. Finally, we stress that Eq. (7) represents a conservative estimate of the change in resistance. In fact, in the regime where $l_\phi > l_{loc}$, i.e. in the Anderson localization regime, the resistance would be highly sensitive to changes in the fractional coverage of active sites. Calculation of the actual resistance of the CNT in this regime would, however, involve a full transport calculation in the presence of

all N impurities. At this point it suffices to see that the conservative estimates obtained from Eq. (7) predict measurable signals in response to small changes in concentration of the target molecules.

To our knowledge, controlled doping of CNTs with transition metal atoms has so far not been achieved. It has, however, been found that metal atoms incorporated into the CNT lattice during catalytic growth are afterwards very difficult to remove [30]. Furthermore, it has been shown that CNT vacancies, which are needed for the metallic doping, may be formed in a controlled way by irradiation by Ar ions [31]. This suggests that metallic doping of CNTs should be possible.

In summary, we have presented a general model of nanostructured chemical sensors which takes the adsorption energies of the relevant chemical species and their individual scattering resistances as the only input. On the basis of this model we have performed a computational screening of transition metal doped CNTs, and found that Ni-doped CNTs are promising candidates for detecting CO in a background of air. The model may be applied straightforwardly to other nanostructures than CNTs, other functionalizations than metal doping and other gas compositions than air.

The authors acknowledge financial support from Spanish MEC (FIS2007-65702-C02-01), “Grupos Consolidados UPV/EHU del Gobierno Vasco” (IT-319-07), e-I3 ETSF project (Contract Number 211956), “Red Española de Supercomputación”, NABIIT and the Danish Center for Scientific Computing. The Center for Atomic-scale Materials Design (CAMD) is sponsored by the Lundbeck Foundation. JMG-L acknowledges funding from Spanish MICINN through Juan de la Cierva and José Castillejo programs.

[8] S. Brahim, S. Colbern, R. Gump, and L. Grigorian, “Tailoring gas sensing properties of carbon nanotubes”, *J. Appl. Phys.* **104**(2), 024502 (Jul. 2008), doi:[10.1063/1.2956395](https://doi.org/10.1063/1.2956395).

[9] C. Morgan, Z. Alemipour, and M. Baxendale, “Variable range hopping in oxygen-exposed single-wall carbon nanotube networks”, *Phys. Stat. Solidi A* **205**(6), 1394 (May 2008), doi:[10.1002/pssa.200778113](https://doi.org/10.1002/pssa.200778113).

[10] D. J. Mowbray, C. Morgan, and K. S. Thygesen, “Influence of O_2 and N_2 on the conductivity of carbon nanotube networks”, *Phys. Rev. B* **79**(19), 195431 (May 2009), doi:[10.1103/PhysRevB.79.195431](https://doi.org/10.1103/PhysRevB.79.195431).

[11] L. Valentini, F. Mercuri, I. Armentano, C. Cantalini, S. Picozzi, L. Lozzi, S. Santucci, A. Sgamellotti, and J. M. Kenny, “Role of defects on the gas sensing properties of carbon nanotubes thin films: experiment and theory”, *Chem. Phys. Lett.* **387**(4-6), 356 (Apr. 2004), doi:[10.1016/j.cplett.2004.02.038](https://doi.org/10.1016/j.cplett.2004.02.038).

[12] Z. Zanolli and J.-C. Charlier, “Defective carbon nanotubes for single-molecule sensing”, *Phys. Rev. B* **80**(15), 155447 (Oct. 2009), doi:[10.1103/PhysRevB.80.155447](https://doi.org/10.1103/PhysRevB.80.155447).

[13] J. M. García-Lastra, K. S. Thygesen, M. Strange, and Ángel Rubio, “Conductance of sidewall-functionalized carbon nanotubes: Universal dependence on adsorption sites”, *Phys. Rev. Lett.* **101**(23), 236806 (Dec. 2008), doi:[10.1103/PhysRevLett.101.236806](https://doi.org/10.1103/PhysRevLett.101.236806).

[14] S. B. Fagan, R. Mota, A. J. R. da Silva, and A. Fazzio, “*Ab initio* study of an iron atom interacting with single-wall carbon nanotubes”, *Phys. Rev. B* **67**(20), 205414 (May 2003), doi:[10.1103/PhysRevB.67.205414](https://doi.org/10.1103/PhysRevB.67.205414).

[15] Y. Yagi, T. M. Briere, M. H. F. Sluiter, V. Kumar, A. A. Farajian, and Y. Kawazoe, “Stable geometries and magnetic properties of single-walled carbon nanotubes doped with 3d transition metals: A first-principles study”, *Phys. Rev. B* **69**(7), 075414 (Feb 2004), doi:[10.1103/PhysRevB.69.075414](https://doi.org/10.1103/PhysRevB.69.075414).

[16] S. H. Yang, W. H. Shin, J. W. Lee, S. Y. Kim, S. I. Woo, and J. K. Kang, “Interaction of a transition metal atom with intrinsic defects in single-walled carbon nanotubes”, *J. Phys. Chem. B* **110**(28), 13941 (Jun. 2006), doi:[10.1021/jp061895q](https://doi.org/10.1021/jp061895q).

[17] K. T. Chan, J. B. Neaton, and M. L. Cohen, “First-principles study of metal adatom adsorption on graphene”, *Phys. Rev. B* **77**, 235430 (Jun. 2008), doi:[10.1103/PhysRevB.77.235430](https://doi.org/10.1103/PhysRevB.77.235430).

[18] C. S. Yeung, L. V. Liu, and Y. A. Wang, “Adsorption of small gas molecules onto Pt-doped single-walled carbon nanotubes”, *J. Phys. Chem. C* **112**(19), 7401 (Apr. 2008), doi:[10.1021/jp0753981](https://doi.org/10.1021/jp0753981).

[19] T. Vo, Y.-D. Wu, R. Car, and M. Robert, “Structures, interactions, and ferromagnetism of Fe-carbon nanotube systems”, *J. Phys. Chem. C* **112**(22), 400 (May 2008), doi:[10.1021/jp0761968](https://doi.org/10.1021/jp0761968).

[20] J. A. Fürst, M. Brandbyge, A.-P. Jauho, and K. Stokbro, “*Ab initio* study of spin-dependent transport in carbon nanotubes with iron and vanadium adatoms”, *Phys. Rev. B* **78**(19), 195405 (Nov. 2008), doi:[10.1103/PhysRevB.78.195405](https://doi.org/10.1103/PhysRevB.78.195405).

[21] A. V. Krasheninnikov, P. O. Lehtinen, A. S. Foster, P. Pyykkö, and R. M. Nieminen, “Embedding transition-metal atoms in graphene: Structure, bonding, and magnetism”, *Phys. Rev. Lett.* **102**(12), 126807 (Mar. 2009), doi:[10.1103/PhysRevLett.102.126807](https://doi.org/10.1103/PhysRevLett.102.126807).

[22] J. J. Mortensen, L. B. Hansen, and K. W. Jacobsen, “Real-space grid implementation of the projector augmented wave method”, *Phys. Rev. B* **71**(3), 035109 (Jan. 2005), doi:[10.1103/PhysRevB.71.035109](https://doi.org/10.1103/PhysRevB.71.035109).

[23] J. P. Perdew, K. Burke, and M. Ernzerhof, “Generalized gradient approximation made simple”, *Phys. Rev. Lett.* **77**(18), 3865 (Oct. 1996), doi:[10.1103/PhysRevLett.77.3865](https://doi.org/10.1103/PhysRevLett.77.3865).

* Electronic address: juanmaria.garcia@ehu.es

[1] *Gas Sensing Materials, MRS Bull.*, vol. 24 (1999).

[2] J. C. Chalier, X. Blase, and S. Roche, “Electronic and transport properties of nanotubes”, *Rev. Mod. Phys.* **79**(2), 677 (May 2007), doi:[10.1103/RevModPhys.79.677](https://doi.org/10.1103/RevModPhys.79.677).

[3] J. Kong, N. R. Franklin, C. Zhou, M. G. Chapline, S. Peng, K. Cho, and H. Dai, “Nanotube molecular wires as chemical sensors”, *Science* **287**(5453), 622 (Jan. 2000), doi:[10.1126/science.287.5453.622](https://doi.org/10.1126/science.287.5453.622).

[4] P. G. Collins, K. Bradley, M. Ishigami, and A. Zettl, “Extreme oxygen sensitivity of electronic properties of carbon nanotubes”, *Science* **287**(5459), 1801 (Mar. 2000), doi:[10.1126/science.287.5459.1801](https://doi.org/10.1126/science.287.5459.1801).

[5] C. Hierold, *Carbon Nanotube Devices: Properties, Modeling, Integration and Applications* (Wiley-VCH, Weinheim, 2008).

[6] F. Villalpando-Páez, A. H. Romero, E. Muñoz-Sandoval, L. M. Martínez, H. Terrones, and M. Terrones, “Fabrication of vapor and gas sensors using films of aligned CN_x nanotubes”, *Chem. Phys. Lett.* **386**(1-3), 137 (Mar. 2004), doi:[10.1016/j.cplett.2004.01.052](https://doi.org/10.1016/j.cplett.2004.01.052).

[7] A. R. Rocha, M. Rossi, A. Fazzio, and A. J. R. da Silva, “Designing real nanotube-based gas sensors”, *Phys. Rev. Lett.* **100**(17), 176803 (May 2008), doi:[10.1103/PhysRevLett.100.176803](https://doi.org/10.1103/PhysRevLett.100.176803).

[24] M. Strange, I. S. Kristensen, K. S. Thygesen, and K. W. Jacobsen, “Benchmark density functional theory calculations for nanoscale conductance”, *J. Chem. Phys.* **128**(11), 114714 (Mar. 2008), doi:[10.1063/1.2839275](https://doi.org/10.1063/1.2839275).

[25] J. M. Soler, E. Artacho, J. D. Gale, A. Garcia, J. Junquera, P. Ordejón, and D. Sánchez-Portal, “The SIESTA method for *ab initio* order-*n* materials simulation”, *J. Phys.: Condens. Matter* **14**(11), 2745 (Mar. 2002), doi:[10.1088/0953-8984/14/11/302](https://doi.org/10.1088/0953-8984/14/11/302).

[26] J. S. Griffith, *The Theory of Transition-Metal Ions* (Cambridge University Press, London, 1961).

[27] P. Atkins and J. de Paula, *Physical Chemistry*, 8th ed. (Oxford University Press, London, 2006).

[28] D. Lide, *Handbook of Chemistry and Physics*, 87th ed. (CRC-Press, 2006–2007).

[29] T. Markussen, R. Rurrali, A.-P. Jauho, and M. Brandbyge, “Scaling theory put into practice: First-principles modeling of transport in doped silicon wires”, *Phys. Rev. Lett.* **99**(7), 076803 (Aug. 2007), doi:[10.1103/PhysRevLett.99.076803](https://doi.org/10.1103/PhysRevLett.99.076803).

[30] M. Ushiro, K. Uno, T. Fujikawa, Y. Sato, K. Tohji, F. Watari, W.-J. Chun, Y. Koike, and K. Asakura, “X-ray absorption fine structure (XAFS) analyses of Ni species trapped in graphene sheet of carbon nanofibers”, *Phys. Rev. B* **73**(14), 144103 (Apr. 2006), doi:[10.1103/PhysRevB.73.144103](https://doi.org/10.1103/PhysRevB.73.144103).

[31] C. Gomez-Navarro, P. J. de Pablo, J. Gomez-Herrero, B. Biel, F. J. Garcia-Vidal, A. Rubio, and F. Flores, “Tuning the conductance of single-walled carbon nanotubes by ion irradiation in the Anderson localization regime”, *Nature Materials* **4**, 534 (Jun. 2005), doi:[10.1038/nmat1414](https://doi.org/10.1038/nmat1414).